

# INFLUENCE OF VEGETATION COVER ON SAND TRANSPORT BY WIND: FIELD STUDIES AT OWENS LAKE, CALIFORNIA

NICHOLAS LANCASTER<sup>1\*</sup> AND ANDY BAAS<sup>2</sup>

<sup>1</sup>*Desert Research Institute, UCCSN, 7010 Dandini Blvd., Reno, NV 89512, USA*

<sup>2</sup>*Visiting from Department of Physical Geography and Soil Science, University of Amsterdam, The Netherlands*

*Received 16 October 1996; Revised 18 March 1997; Accepted 29 April 1997*

## ABSTRACT

Field studies conducted at Owens Lake, California, provide direct measurements of sand flux on sand sheets with zero to 20 per cent cover of salt grass. Results from 12 different sand transport events show that aerodynamic roughness length and threshold wind shear velocity increase with vegetation cover as measured by vertically projected cover and roughness density ( $\lambda$ ). This results in a negative exponential decrease in sediment flux with increasing vegetation cover such that sand transport is effectively eliminated when the vertically projected cover of salt grass is greater than 15 per cent. A general empirical model for the relation between sand flux and vegetation cover has been derived and can be used to predict the amount of vegetation required to stabilize sand dune areas. © 1998 John Wiley & Sons, Ltd.

*Earth surf. process. landforms*, **23**, 69–82 (1998)

KEY WORDS: sand transport; vegetation cover; saltation threshold; wind erosion.

## INTRODUCTION

Vegetation plays an important role in determining the dynamics and morphology of desert and coastal sand dune environments via its influence on the entrainment and transport of sand by the wind (Musick and Gillette, 1990; Tsoar and Møller, 1986; Wiggs *et al.*, 1994, 1995, 1996; Wolfe and Nickling, 1993). Quantification of the effect of vegetation on sediment transport can be used to assess the effects of climatic change and human disturbance on such areas, as well as aiding sand stabilization and environmental restoration efforts.

Vegetation protects the surface via direct cover of the surface, trapping of particles, and most importantly by extracting momentum from the air flow (Wolfe and Nickling, 1993). When the wind blows over a smooth unobstructed surface, shear stress acts more or less uniformly across the entire surface, but when non-erodible roughness elements are present a proportion of the shear stress is absorbed by the roughness elements on the underlying erodible surface. The degree of protection is a function of their size, geometry and spacing (Lyles *et al.*, 1974; Marshall, 1971; Musick and Gillette, 1990; Stockton and Gillette, 1990). Low densities of roughness elements tend to reduce the threshold velocity of the surface and cause increased erosion around the elements because of the development and shedding of eddies (Logie, 1982). By contrast, higher densities of roughness elements tend to increase the threshold velocity of the surface. Field and wind tunnel experiments suggest that the most important influence of vegetation cover is via the threshold wind shear velocity for transport ( $u_{*t}$ ) (Musick and Gillette, 1990; Musick and Trujillo, 1996; Wolfe and Nickling, 1996).

Although many sand surfaces are vegetated to some degree, the effects of vegetation on sand transport rates are poorly known. Studies in Australia indicate that sand transport can take place even when vegetation cover is as much as 45 per cent (Ash and Wasson, 1983; Wasson and Nanninga, 1986). Investigations of the effects of vegetation on dune dynamics in the Kalahari indicate large changes in erosion and deposition rates when vegetation is reduced (Wiggs *et al.*, 1994). Wind tunnel studies provide important data on the effects of artificial cover on transport and erosion rates (e.g. Bilbro and Fryrear, 1994; Buckley, 1987; Fryrear, 1985) and threshold wind shear velocity (Musick and Trujillo, 1996).

\* Correspondence to: N. Lancaster

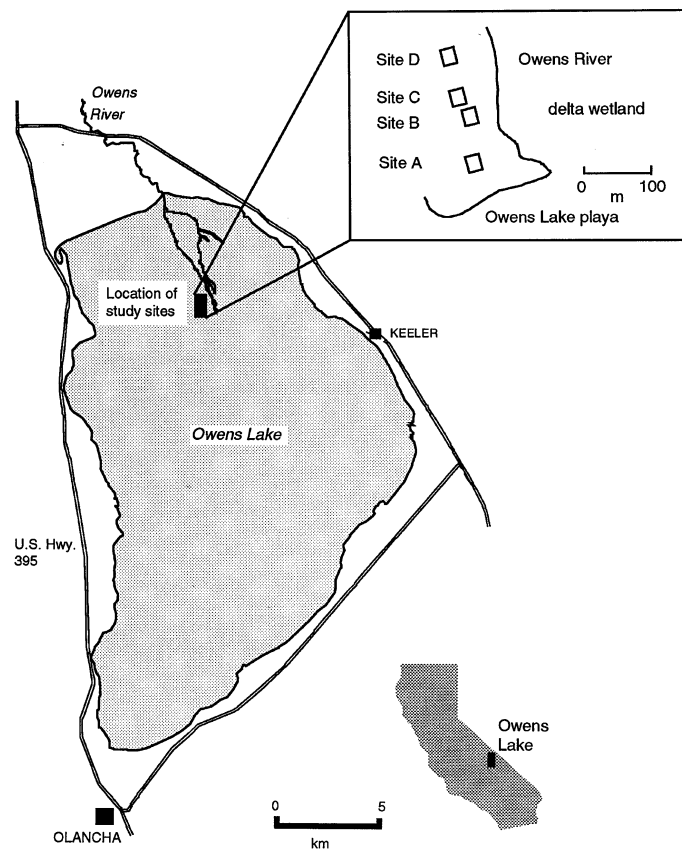


Figure 1. Location map showing Owens Lake and the location of the study sites

We report here the results of field studies conducted at Owens Lake, California, that provide direct measurements of sand flux on sparsely vegetated sand surfaces and provide quantification of the effect of vegetation on sand transport by wind.

### FIELD SITES

The studies were conducted on the western part of the former delta of the Owens River in eastern California (Figure 1). The area is characterized by a coarse sand sheet developed by wind reworking of fluvial/deltaic sands deposited prior to the lowering of Owens Lake by diversion of water to the Los Angeles aqueduct since the 1920s. The sand sheets are vegetated with salt grass (*Distichlis spicata*) with a cover that ranges from zero to about 30 per cent and which increases northwards away from the edge of the bare playa surface of Owens Lake.

Four 40 m by 15 m plots were established spanning a range of vegetation cover density from bare to moderate (Sites A to D). Total relief on each of the plots was less than 1 m and ranged between 0.14 m at Site A to 0.80 m at Sites C and D. Site A was a smooth, bare, wind-rippled sand surface with a slope from south to north and a total relief of 0.14 m (Figure 2a). Site B was within a wide blowout and sloped slightly to the north (Figure 2b). Site C had the greatest local relief with many small (0.30–0.50 m high) sand mounds around clumps of salt grass (Figure 2c). Local relief at Site D (Figure 2d) was less pronounced, with broad undulations 0.2 m to 0.6 m high. The surface sand at all sites is coarse (median particle size 0.1–1.0 phi; 1000–500 µm), moderately to poorly sorted (Folk graphic standard deviation 0.90–1.34 phi), and strongly fine-skewed (phi skewness 0.40–0.65). Representative particle size distributions are shown in Figure 3.

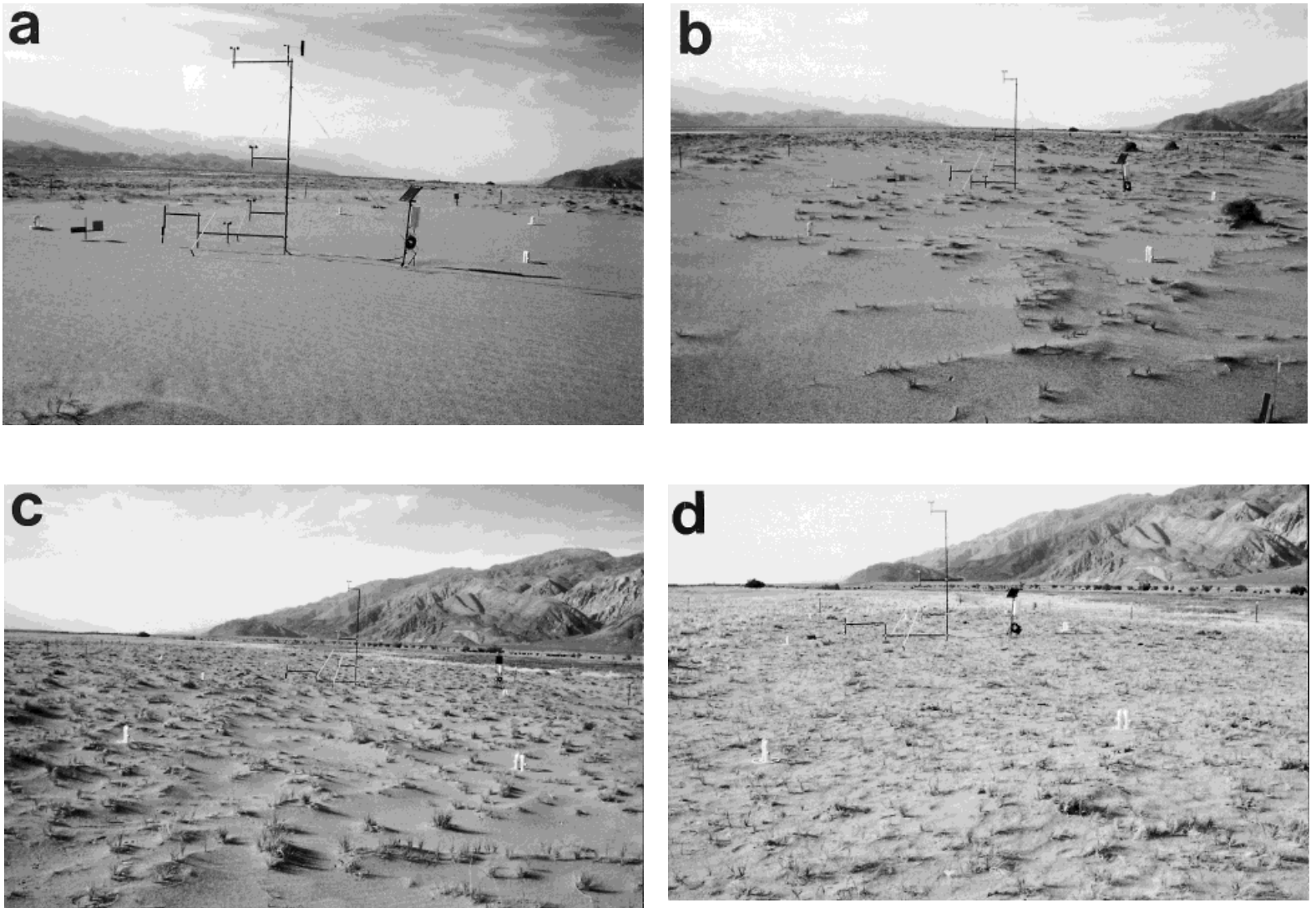


Figure 2. The study sites (all views looking north or northwest): (a) Site A, (b) Site B, (c) Site C, (d) Site D

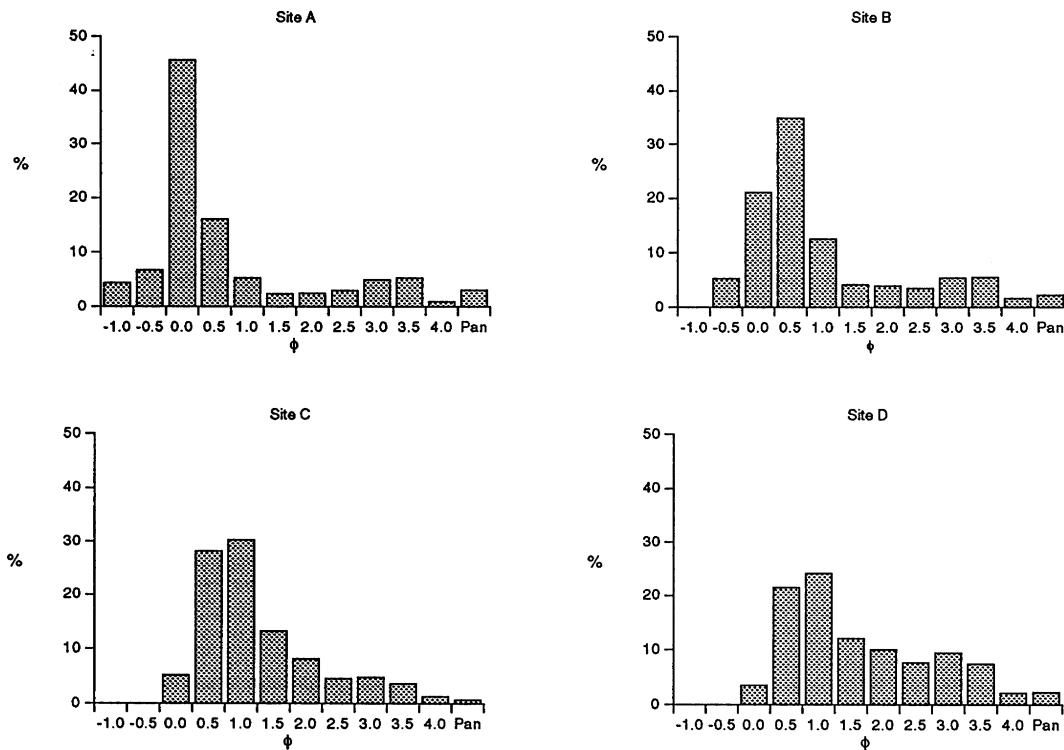


Figure 3. Particle size distributions for surface sand at study sites

Each plot was instrumented from early November 1995 to May 1996 with eight bidirectional sand collectors at a height of 0.1 m as used elsewhere at Owens Lake by the Great Basin Unified Air Pollution Control District (Ono *et al.*, 1994); a mast with four Met One cup anemometers, spaced logarithmically at heights of 0.5, 1.0, 2.0 and 4.0 m; a piezo-electric sensor to detect the onset of sand transport (a Sensit; Stockton and Gillette, 1990) at a height of 0.2 m, and a BSNE sand trap (Fryrear, 1986) at 0.2 m height. The anemometer mast at Site A was also equipped with a wind vane. The instrument layout is shown schematically in Figure 4. Wind speed and direction were sampled every 2 s and were recorded on a 1 h average for most of the time, but a 5 min interval for periods during which the wind speed exceeded  $8 \text{ m s}^{-1}$  at the two highest anemometers. The Sensit data were recorded as 5 min total counts of saltation impacts.

### VEGETATION COVER AND GEOMETRY

The effect of vegetation on the wind and sediment transport can be assessed by estimating or measuring the plant silhouette area (the vertical cross-section of the plant that the wind 'sees',  $A_s$ ) and density to produce a measure of roughness density  $\lambda$  (Raupach *et al.*, 1993), or in the case of vegetation, the lateral cover ( $L_c$ ) (Musick and Gillette, 1990). Both parameters are defined as the ratio between silhouette area (the cross-section of the plant that the wind 'sees') and total surface area:

$$L_c = DA_s \quad (1)$$

where  $D$  is canopy population density (number of individuals per unit area) and  $A_s$  is mean frontal-silhouette area (height  $\times$  diameter) per canopy, and:

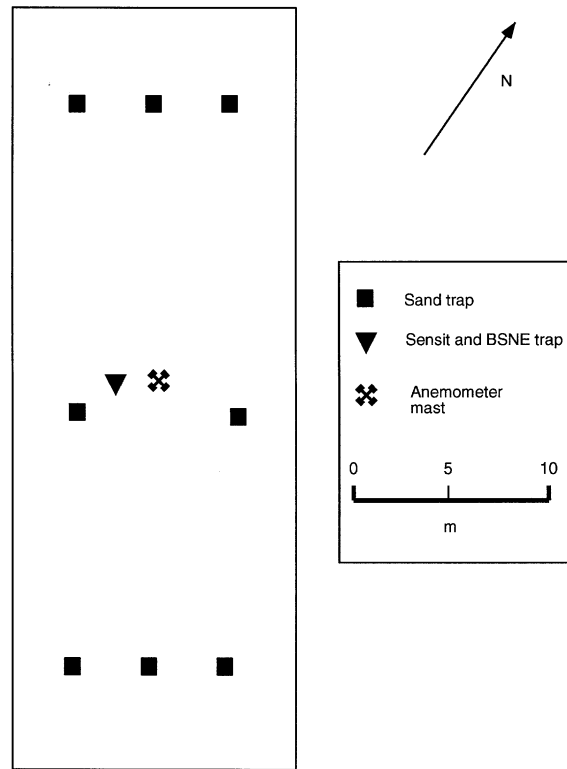


Figure 4. Schematic diagram of instrument and sand trap layout at study sites

$$\lambda = A_s / S \quad (2)$$

where  $S$  is the surface area per plant.

For sparse arrays, the aerodynamic roughness can be approximated by

$$z_0 = \lambda H \quad (3)$$

where  $H$  is the mean height of the roughness elements (Raupach *et al.*, 1993).

The effect of vegetation on threshold wind shear velocity can be described by the ratio between the threshold wind shear velocity with and without roughness elements (Raupach *et al.*, 1993):

$$u_{*t}/u_{*tr} = (1 - m\alpha L_c)^{0.5} (1 + M\beta L_c)^{0.5} \quad (4)$$

where  $\beta$  is the ratio of the drag coefficient of an isolated roughness element on the surface to the drag coefficient of the surface itself,  $\alpha$  is the basal to frontal area ratio of the roughness elements, and  $m$  is a parameter that describes the difference between the average and maximum shear stress on the surface.

Vegetation cover was surveyed in mid-November 1995 and again in early May 1996. No significant growth occurred between these dates as the grass was in its winter dormant stage. Two 40 m long transects parallel to the site axis were laid out on each site, 4 m and 12 m from its west edge. One metre square quadrats were laid out at alternate metre points along the transect, giving a total of 20 quadrats per transect and 40 quadrats per site. Within each plot, salt grass clumps were counted ( $n$ ) and measured for maximum height ( $h$ ), length of longest axis ( $l$ ), and length of the perpendicular axis ( $w$ ). A clump was included in the data if a portion of it was rooted within the plot. The roughness density for each site was calculated as:

$$\Sigma \{nh[(wl)/2]/a\} \quad (5)$$

where  $a$  is the area of each quadrat ( $1 \text{ m}^2$ ). No distinction was made between live, dormant and dead stems. The

Table I. Summary of vegetation characteristics at study sites

Site	Roughness density ( $\lambda$ )	Height (m)	Cover (%)
B	0.0395	0.10	4.2
C	0.0948	0.09	12.0
D	0.2120	0.11	26.3

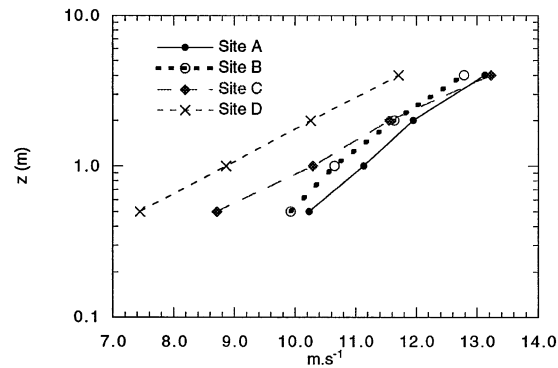


Figure 5. Representative simultaneous wind velocity profiles for each site (27 November 1995)

Table II. Hourly mean values of wind shear velocity and aerodynamic roughness length

Site	Mean $u_*$ ( $\text{m s}^{-1}$ )	Mean aerodynamic roughness length (m)
A	0.3840	0.00075
B	0.4216	0.00200
C	0.5317	0.00788
D	0.5982	0.01321

percentage vegetation cover was calculated as:

$$\Sigma (wl)/a \quad (6)$$

Data on vegetation cover are summarized in Table I. The lateral cover of salt grass ranged between zero at Site A and 0.2120 at Site D. This corresponds to a range in vertically projected vegetation cover of 0 to 26.3 per cent.

### BOUNDARY-LAYER WINDS

Wind data were initially sorted by wind speed at the lowest anemometer (0.5 m) and a subset of the data in which the wind speed at the lowest anemometer exceeded  $4 \text{ m s}^{-1}$  was extracted. In the absence of temperature measurements, this was done to minimize the effects of thermal instability of the atmosphere, and to obtain data for wind speeds at which mechanical turbulence exceeded buoyancy effects (Lancaster *et al.*, 1991; Wolfe and Nickling, 1996). These data were used for subsequent calculations of aerodynamic roughness ( $z_0$ ) and wind shear velocity ( $u_*$ ) using a least-squares fit to the data. Thus, given a linear fit of the form  $y = mx + b$ , where  $y = \ln(z) = u_{(z)}$ ,  $b = \ln(z_0)$  and  $m = \kappa/u_*$ :

$$u_* = \kappa/m \quad (7)$$

and

$$z_0 = e^b \quad (8)$$

where  $\kappa$  is the von Karmann constant (0.4).

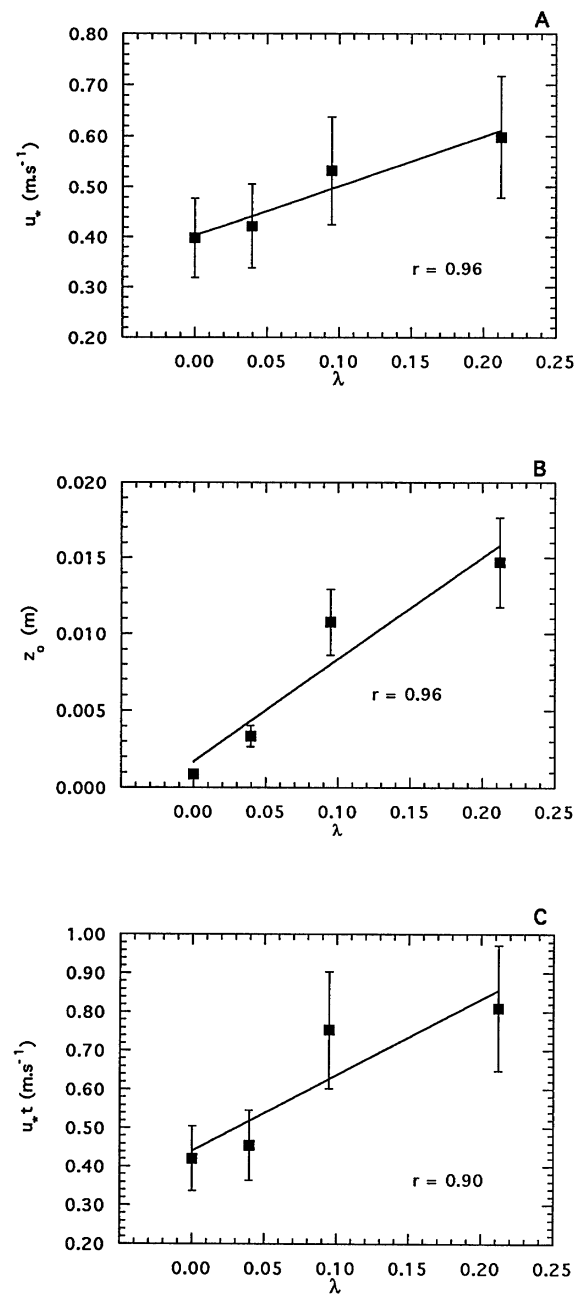


Figure 6. Relations between roughness density and mean values of (A) wind shear velocity, (B) aerodynamic roughness, (C) and threshold wind shear velocity. Error bars are  $\pm 10$  per cent of mean value

We did not use a form of the Prandtl–von Karmann equation that incorporates a displacement height because we wished to compare data from vegetated and unvegetated surfaces. The excellent fit of the wind profile data to the Prandtl–von Karmann equation with the displacement height set to zero suggests, however, that the actual displacement height was negligible.

Several checks were placed on the calculations of wind profile parameters following the methods outlined by Bauer *et al.* (1992). For each profile, the least-squares error (normalized to  $r^2$ , the coefficient of determination)

Table III. Comparison of aerodynamic roughness values with and without sand transport

Site	Mean $z_0$ (m)	St. dev.	Mean $z_{0t}$ (m)	St. dev.
A	0.00090	0.00409	0.00128	0.00200
B	0.00334	0.00874	0.00293	0.00261
C	0.01078	0.01291	0.02002	0.01343
D	0.01471	0.01425	0.01758	0.01492

Table IV. Threshold wind shear velocity values ( $\text{m s}^{-1}$ ) for start and end of sand transport events

Site	$u_{*t}$ start	$u_{*t}$ end	$u_{*t}$ combined
A	0.4194	0.4211	0.4207
B	0.4609	0.4474	0.4546
C	0.7611	0.7432	0.7529
D	0.8146	0.8031	0.8094

was calculated for the estimates of  $z_0$  and  $u_*$ . The maximum acceptable error in estimating  $z_0$  was set at 5 per cent. Profiles for which the error exceeded this limit were rejected.

Representative simultaneous wind profiles for each site are shown in Figure 5 and wind profile parameters are summarized in Table II. Wind shear velocity and aerodynamic roughness increase with vegetation cover from Site A to Site D. Hourly averages of wind shear velocity increase from  $0.3840 \text{ m s}^{-1}$  at Site A to  $0.5982 \text{ m s}^{-1}$  at Site D. The 5 min averages of wind shear velocity are slightly higher, because they represent periods during which winds were generally stronger, but show a similar increase from  $0.3984 \text{ m s}^{-1}$  at Site A to  $0.6430 \text{ m s}^{-1}$  at Site D. There are strong positive relations between average  $u_*$ , roughness density ( $\lambda$ ) and vegetation cover ( $r^2=0.92, 0.94$  respectively) (Figure 6A).

#### *Aerodynamic roughness*

Because there is a saltation layer of sand above the surface during transport events, values of aerodynamic roughness ( $z_0$ ) may vary, depending on whether or not there is sand transport. The initial data set was therefore divided into intervals with and without sand transport, based on the current  $u_*$  and the Sensit count. The data set for intervals without sand transport includes intervals in which both the  $u_*$  value is less than the threshold wind shear velocity ( $u_{*t}$ ) for each plot ( $u_* < u_{*t}$ ) and the Sensit detects no particles (count=0). Intervals during which both  $u_*$  exceeds  $u_{*t}$  and the Sensit detects particles (count>0), form the second data set. Average  $z_0$  values for each plot were calculated under transport ( $z_{0t}$ ) and non-transport conditions ( $z_0$ ) (Table III). Mean values of aerodynamic roughness length range between  $0.00090 \text{ m}$  for Site A and  $0.01471 \text{ m}$  for Site D. There was, however, no statistically significant difference between  $z_0$  and  $z_{0t}$  for the vegetated sites ( $t$ -test, 0.05 significance level). This suggests that the aerodynamic roughness due to the vegetation cover overwhelms that due to the saltating sand (Owen, 1964). There are strong positive relations between the aerodynamic roughness length, roughness density, and vegetation cover ( $r^2=0.91, 0.93$  respectively) as shown in Figure 6B.

#### *Threshold wind shear velocity*

The threshold wind shear velocity for sediment transport was determined by identifying the 5 min intervals at which the Sensit started and ended recording particle movement. The  $u_*$  value for these intervals was considered to be the threshold shear velocity at the start and end of sand transport. Averaging these  $u_*$  values over the whole data set gives a mean  $u_{*t}$  at the start and end of transport (' $u_{*t}$  start', ' $u_{*t}$  end') (Table IV). These values for  $u_{*t}$  were found to differ by an amount that was not statistically significant and therefore all values of  $u_{*t}$  were averaged to give a representative value (' $u_{*t}$  combined').

Values of  $u_{*t}$  range between  $0.4207 \text{ m s}^{-1}$  at Site A and  $0.8094 \text{ m s}^{-1}$  at Site D. The value for the bare sand site compares well with the value for threshold velocity calculated using the equation of Bagnold (1941), which is  $0.49 \text{ m s}^{-1}$  for a sand with a modal diameter of  $1000 \mu\text{m}$ . There are strong positive relations between the threshold wind shear velocity for sand transport, roughness density, and vegetation cover ( $r^2=0.81, 0.83$  respectively) as shown in Figure 6C.



Table V. Sand flux ( $\text{g m}^{-2} \text{s}^{-1}$ ) for northwesterly and southerly wind events

Event No.	Date	Sand flux			
		Site A	Site B	Site C	Site D
1n	30/11/95	0.0167	0.0104	0.0023	0.0007
3n	18/12/95	0.0762	0.0131	0.0019	0.0001
4n	2/1/96	0.5083	0.1598	0.0084	0.0011
5n	22/1/96	0.0237	0.0126	0.0022	0.0000
6n	26/1/96	0.1465	0.0418	0.0082	0.0001
8n	25/3/96	0.2188	0.1488	0.1445	0.0194
9n	27/3/96	3.8888	2.2558	0.7096	0.0712
10n	31/3/96	0.8832	0.3953	0.2021	0.1391
11n	30/4/96	0.1870	0.1023	0.2633	0.1406
2s	13/12/95	1.4842	2.0965	0.3510	0.0152
3s	18/12/95	0.1407	0.1058	0.0431	0.0006
5s	22/1/96	0.0123	0.0101	0.0037	0.0000
7s	25/2/96	0.4004	0.3340	0.3190	0.0028
8s	25/3/96	0.6616	0.3363	0.4887	0.1019
10s	31/3/96	0.0431	0.2253	nd	nd
11s	30/4/96	0.4535	0.4091	0.3983	0.0130

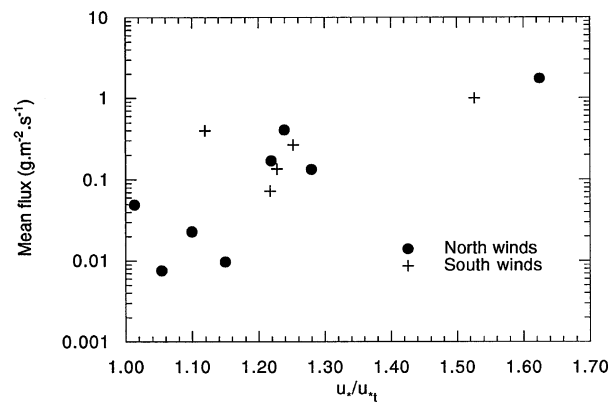


Figure 7. Relations between magnitude of sand transport event (as measured by the mean sand flux) and the ratio between mean wind shear velocity and threshold wind shear velocity (measured at Site A)

### SEDIMENT FLUX

The sand collectors and BSNE trap were emptied following each major wind and sand transport event. A total of 16 data sets were obtained in this way, 12 of which were selected for further analysis. The mass of sand caught in each of the eight collectors was averaged to provide a mean sand catch per plot and event. The mean within-plot coefficient of variability of the sand catch ranged between 33 and 42 per cent for sites A, B and D. Site C was the most variable, with a 56 per cent variability.

To provide an estimate of sediment flux, the total sand catch for each major wind direction sector (northwesterly and southerly) was divided by the time represented by the 5 min intervals when the Sensit count exceeded 0 and the wind was from a 90 degree sector centred on that direction ( $326^\circ$  and  $146^\circ$  respectively). The sediment flux is expressed as (grams per metre squared per second). Mean values are given in Table V.

The overall magnitude of the event as described by the average sediment flux increases as a power function of the ratio between the average  $u_*$  value for the event and the threshold for bare sand at Site A (Figure 7). There is a strong exponential decrease in sand flux with vegetation cover and roughness density for both northerly and southerly winds (Figure 8). The nature of the relations between sediment flux and vegetation cover does, however, vary somewhat between wind directions. During southerly winds, the sand moves from areas of lower to higher vegetation cover. Flux decreases by only 10 to 20 per cent from Site A to Site B, and then declines

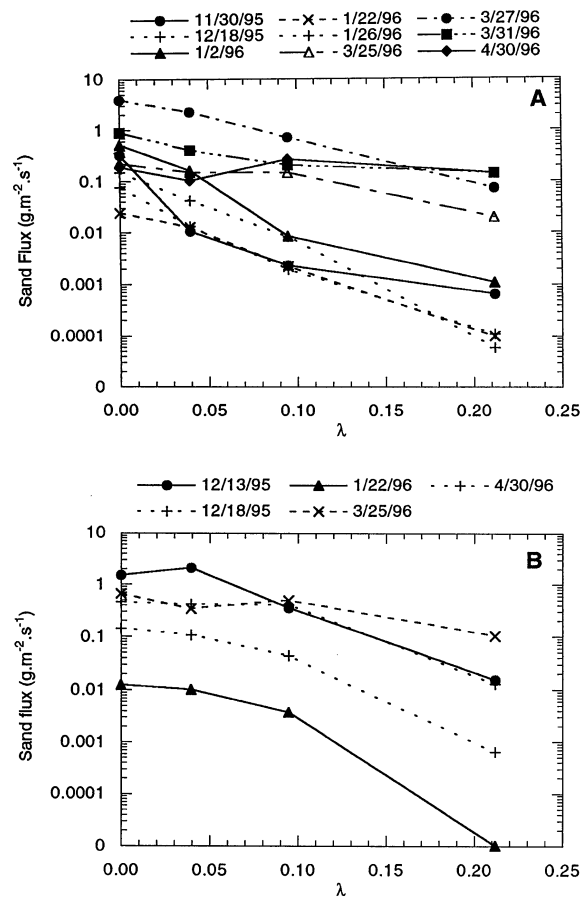


Figure 8. Relations between sediment flux and roughness density: (A) northwesterly winds, (B) southerly winds

sharply to 20 to 30 per cent of the bare sand value at Site C. This condition is probably a 'fetch effect' (Gillette *et al.*, 1996) in which the decrease of sand flux with distance is less rapid than the parallel change in wind shear velocity. During northwesterly wind events, sand moves from areas of higher to lower vegetation cover. Transport at Site C is 10 per cent of the bare sand value, and is 46 per cent of this amount at Site B. In both situations, the flux at Site D is typically only 3–4 per cent of the bare sand amount.

Insight into possible fetch effects can be gained by examining the within-site variability in sand flux (Figure 9). For northwesterly wind events, sand flux increases from north to south within each plot, so that the maximum flux is recorded at the south end of Site A. Conversely, for southerly wind events, there is initially an increase in flux at Site A, as the wind moves from the playa surface to the sand sheet. The maximum flux is recorded at the north end of Site A, or the south end of Site B. Thereafter, sand flux decreases from south to north within each plot.

The relations between sand flux and vegetation cover can be modelled as a negative exponential function of roughness density using a simple expression for sand flux as  $(u_* - u_{*t})^3$ , where  $u_*$  is the mean  $u_*$  for the site and  $u_{*t}$  is the threshold for transport on a bare sand surface. The modelled sand flux ( $q$ ) as a function of roughness density ( $\lambda$ ) is given as:

$$q = 300 (u_* - u_{*t})^3 e^{-25\lambda} \quad (9)$$

Figure 10 shows the generally good agreement that is obtained between modelled and measured values of sand flux as a function of roughness density ( $\lambda$ ).

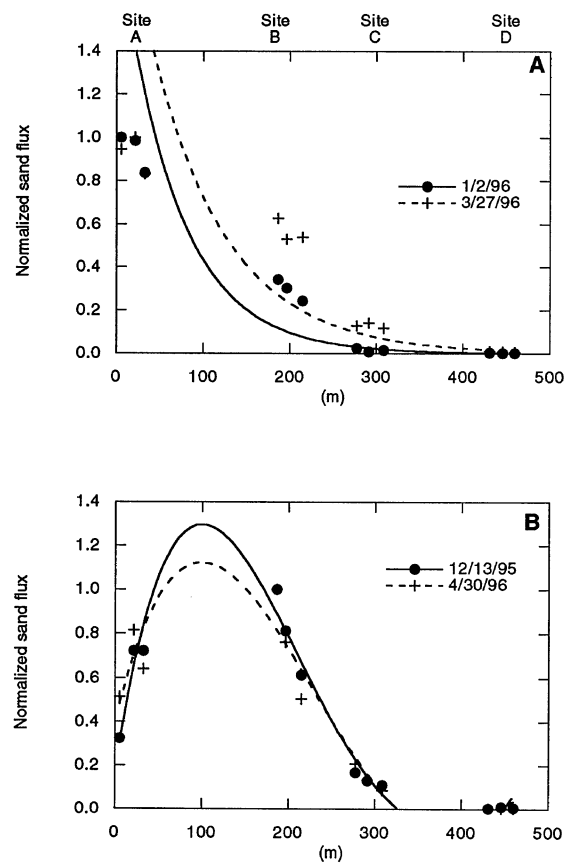


Figure 9. Changes in sand flux with distance for representative northwesterly (A) and southerly (B) events. Third-order polynomial fitted to data. Note that for southerly winds, maximum flux appears to be reached between Sites A and B

## DISCUSSION

The presence of vegetation on sand sheet surfaces on the Owens River delta acts to increase the threshold wind shear velocity for transport by a factor of almost two in comparison with adjacent unvegetated surfaces. Despite increases in average wind shear velocity with increasing vegetation cover, sand flux decreases exponentially with vegetation cover because of the strong influence of vegetation on transport threshold.

The effect of vegetation cover on threshold can be quantified by the threshold  $u_*$  ratio ( $R$ ), or the ratio of the threshold wind shear velocity between a surface without and with roughness elements (Musick and Gillette, 1990) (Table VI). Values of the threshold shear velocity ratio decrease with vegetation cover, as predicted by the experimental and model data (Raupach *et al.*, 1993). Values of  $R$  for the study sites are higher than predicted by Raupach's model and those reported for sites with a similar roughness density studied by Musick and Gillette (1990) and Wolfe and Nickling (1996) (Figure 11). The field data, however, lie within the range of values determined for arrays of porous roughness elements in wind tunnel experiments by Musick and Trujillo (1996). These comparisons indicate that the cover of vegetation has less effect on threshold than would be predicted from model data and probably reflects the influence of vegetation structure and porosity (shrubs versus grass) on the threshold  $u_*$  ratio.

The model and field results can also be used to predict the amount of salt grass vegetation required to reduce sand transport to desired values. By graphing the normalized sand flux against vegetation cover, it is possible to determine the vegetation cover that reduces sand flux to certain levels (Figure 12). The empirical relation can be expressed as a predictive equation of the form:

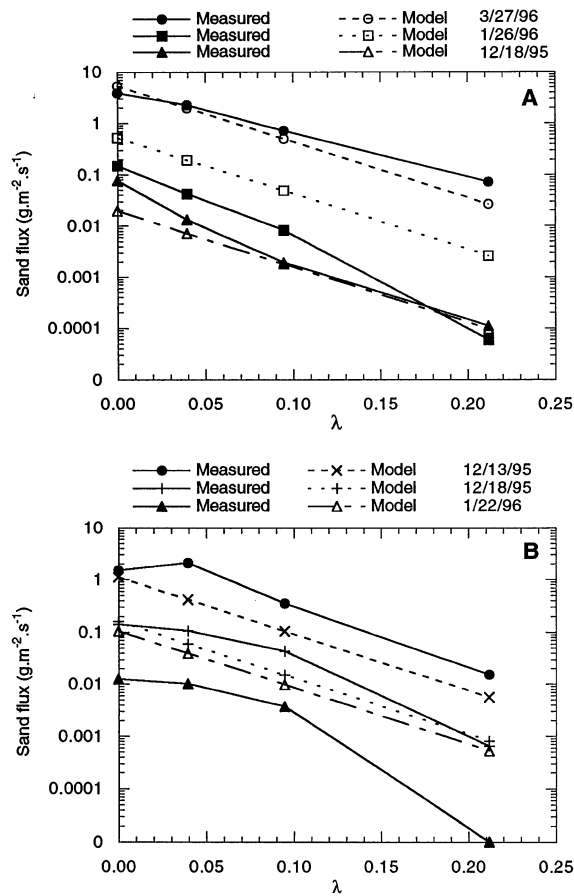


Figure 10. Comparison between model and measured sand transport rates for representative events: (A) northwesterly winds, (B) southerly winds

Table VI. Comparison of calculated (bare sand) and measured  $u_{*t}$  values ( $\text{ms}^{-1}$ )

Site	Measured $u_{*t}$	Calculated $u_{*t}$ (bare sand)	Threshold $u_{*t}$ ratio ( $R$ )
A	0.4207	0.4860	—
B	0.4546	0.4095	0.91
C	0.7529	0.3437	0.46
D	0.8094	0.3437	0.43

$$Qn = 0.95 e^{-0.20c} \quad (10)$$

where  $Qn$  is the sand flux normalized with respect to an equivalent unvegetated sand surface and  $C$  is the percentage vegetation cover.

In the case of the Owens Delta sites, sand flux is reduced to 10 per cent of the equivalent bare sand amount when the cover of salt grass exceeds approximately 12 per cent and to 5 per cent of the bare sand amount when the vegetation cover is 17.5 per cent. These data can be compared with those of Wasson and Nanninga (1986), who suggested that sand transport could occur even with a vegetation cover of as much as 45 per cent. These differences may be the result of plant geometry so that isolated, but relatively large, shrubs or clumps of grass act to increase wind shear velocity and sediment transport in intervening areas, compared to the more even distribution of small salt grass clumps which affect the wind throughout the area.

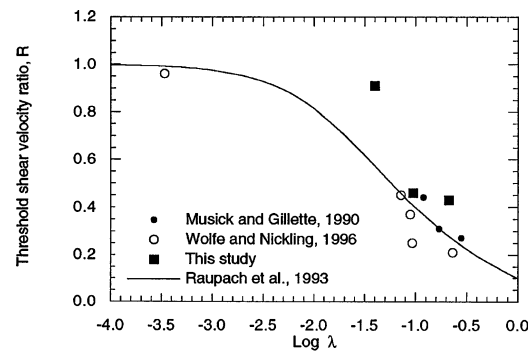


Figure 11. Comparison between threshold shear velocity ratio obtained in this study and data from prior studies

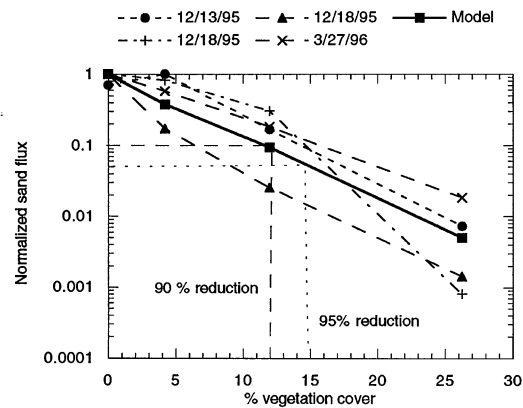


Figure 12. Relations between normalized measured and modelled sand flux and percentage vegetation cover, illustrating the amount of salt grass vegetation required to reduce sand transport by selected amounts

A further comparison can be made with the data of Musick and Gillette (1990), who defined a critical value of the threshold  $u_*$  ratio ( $R$ ) that would protect the surface from erosion. Given that winds with a value of  $1.0 \text{ m s}^{-1}$  represent a limiting case, and a bare sand threshold of approximately  $0.4 \text{ m s}^{-1}$ , the critical value of  $R$  is 0.4, which corresponds in their model to a roughness density of 0.13, or a vegetation cover on the study sites of 16 per cent. The empirical approach adopted here is therefore directly comparable with the theoretical approach of Musick and Gillette (1990).

## CONCLUSIONS

Field studies of the relations between grass cover and sand transport rates show that sand flux decreases exponentially with vegetation cover. They provide further evidence of the strong influence of plant cover on threshold velocity and therefore sediment transport rates. Further studies are required to determine the influence of sediment particle size and plant structure on transport rates before a generally applicable predictive model can be developed. This model could be used to assess the effects of human disturbance and climatic change on the stability of vegetated sand surfaces via changes in plant cover.

## ACKNOWLEDGEMENTS

This study was funded by a contract from the Great Basin Air Pollution Control District. The research was made possible by the support and assistance of Carla Scheidlinger and Jim Paulus and the field work of Chris Rumm and Jeff Smith of the GBUAPCD staff. Wind data reduction was carried out at DRI by Steve Metzger, who also

helped with surveying and other duties. We thank the two reviewers for their constructive comments on the manuscript.

#### REFERENCES

- Ash, J. E. and Wasson, R. J. 1983. 'Vegetation and sand mobility in the Australian desert dunefield', *Zeitschrift für Geomorphologie Supplementband*, **45**, 7–25.
- Bagnold, R. A. 1941. *The Physics of Blown Sand and Desert Dunes*, Chapman and Hall, London.
- Bauer, B. O., Sherman, D. J. and Wolcott, J. F. 1992. 'Sources of uncertainty in shear stress and roughness length estimates derived from velocity profiles', *Professional Geographer*, **44**, 453–464.
- Bilbro, J. D. and Fryrear, D. W. 1994. 'Wind erosion losses as related to plant silhouette and soil cover', *Agronomy Journal*, **88**, 550–553.
- Buckley, R. 1987. 'The effect of sparse vegetation cover on the transport of dune sand by wind', *Nature*, **325**, 426–428.
- Fryrear, D. W. 1985. 'Soil cover and wind erosion', *Transactions, American Society of Agricultural Engineers*, **28**, 781–784.
- Fryrear, D. W. 1986. 'A field dust sampler', *Journal of Soil and Water Conservation*, **41**, 117–120.
- Gillette, D. A., Herbert, G., Stockton, P. H. and Owen, P. R. 1996. 'Causes of the fetch effect in wind erosion', *Earth Surface Processes and Landforms*, **21**, 641–660.
- Lancaster, N., Rasmussen, K. R. and Greeley, R. 1991. 'Interactions between unvegetated desert surfaces and the atmospheric boundary layer: a preliminary assessment', *Acta Mechanica*, Supplementum 2, 89–102.
- Logie, M. 1982. 'Influence of roughness elements and soil moisture of sand to wind erosion', *Catena Supplement*, **1**, 161–173.
- Lyles, L., Schrandt, R. L. and Schneider, N. F. 1974. 'How aerodynamic roughness elements control sand movement', *Transactions, American Society of Agricultural Engineers*, **17**, 134–139.
- Marshall, J. K. 1971. 'Drag measurements in roughness arrays of varying densities and distribution', *Agricultural Meteorology*, **8**, 269–292.
- Musick, H. B. and Gillette, D. A. 1990. 'Field evaluation of relationships between a vegetation structural parameter and sheltering against wind erosion', *Land Degradation and Rehabilitation*, **2**, 87–94.
- Musick, H. B. and Trujillo, S. M. 1996. 'Wind-tunnel modelling of the influence of vegetation structure on saltation threshold', *Earth Surface Processes and Landforms*, **21**, 589–606.
- Ono, D. M., Knop, M. F. and Parker, J. 1994. 'Instruments and techniques for measuring wind-blown dust and PM10 at Owens Lake, California', *Proceedings of the Annual Meeting of the Air and Waste Management Association*, Paper 94-FA145.05.
- Owen, P. R. 1964. 'Saltation of uniform grains in air', *Journal of Fluid Mechanics*, **20**, 225–242.
- Raupach, M. R., Gillette, D. A. and Leys, J. F. 1993. 'The effect of roughness elements on wind erosion threshold', *Journal of Geophysical Research*, **98**, 3023–3029.
- Stockton, P. H. and Gillette, D. A. 1990. 'Field measurements of the sheltering effect of vegetation on erodible land surfaces', *Land Degradation and Rehabilitation*, **2**, 77–86.
- Tsoar, H. and Møller, J. T. 1986. 'The role of vegetation in the formation of linear sand dunes', in Nickling, W. G. (Ed.), *Aeolian Geomorphology*, Allen and Unwin, Boston, 75–95.
- Wasson, R. J. and Nanninga, P. M. 1986. 'Estimating wind transport of sand on vegetated surfaces', *Earth Surface Processes and Landforms*, **11**, 505–514.
- Wiggs, G. F. S., Livingstone, I., Thomas, D. S. G. and Bullard, J. E. 1994. 'Effect of vegetation removal on airflow patterns and dune dynamics in the southwestern Kalahari Desert', *Land Degradation and Rehabilitation*, **5**, 13–24.
- Wiggs, G. F. S., Thomas, D. S. G., Bullard, J. E. and Livingstone, I. 1995. 'Dune mobility and vegetation cover in the southwest Kalahari Desert', *Earth Surface Processes and Landforms*, **20**, 515–530.
- Wiggs, G. F. S., Livingstone, I., Thomas, D. S. G. and Bullard, J. E. 1996. 'Airflow and roughness characteristics over partially vegetated linear dunes in the southwest Kalahari Desert', *Earth Surface Processes and Landforms*, **21**, 19–34.
- Wolfe, S. A. and Nickling, W. G. 1993. 'The protective role of sparse vegetation in wind erosion', *Progress in Physical Geography*, **17**, 50–68.
- Wolfe, S. A. and Nickling, W. G. 1996. 'Shear stress partitioning in sparsely vegetated desert canopies', *Earth Surface Processes and Landforms*, **21**, 607–620.